



Purton, J. A., & Allan, N. L. (2015). Multi-million atom Monte Carlo simulation of oxide materials and solid solutions. *Computational Materials Science*, 103, 244-249.
<https://doi.org/10.1016/j.commatsci.2015.03.016>

Peer reviewed version

Link to published version (if available):
[10.1016/j.commatsci.2015.03.016](https://doi.org/10.1016/j.commatsci.2015.03.016)

[Link to publication record in Explore Bristol Research](#)
PDF-document

University of Bristol - Explore Bristol Research

General rights

This document is made available in accordance with publisher policies. Please cite only the published version using the reference above. Full terms of use are available:
<http://www.bristol.ac.uk/red/research-policy/pure/user-guides/ebr-terms/>

Multi-Million Atom Monte Carlo Simulation of Oxide Materials and Solid Solutions

John A Purton^{a*} and Neil L Allan^b

a. Daresbury Laboratory, STFC, Keckwick Lane, Daresbury, Warrington, WA4 4AD, UK. e-mail: john.purton@stfc.ac.uk, telephone: +44 1925 603785

b. School of Chemistry, Cantock's Close, University of Bristol, Bristol, BS8 1TS, UK. e-mail: n.l.allan@bris.ac.uk, telephone: +44 117 928 8308.

*corresponding author

Abstract

We propose a method for the simulation of large ionic systems with long-range forces using the Monte Carlo method. This method employs a domain decomposition strategy for subdividing the simulation cell and parallelisation of these subdomains using a thread based strategy. This is thus ideally suited to modern day multi-core architectures.

Evaluation of the long range interactions that is incompatible with a domain decomposition strategy has been replaced by the direct calculation of the Coulomb sum [C.J. Fennell and J.D. Gezelter, *J. Chem. Phys.*, 124:234104, 2006.]. We compare this approach with that of "standard" Monte Carlo simulations that employ the Ewald technique. A relatively large two-body cutoff is required to reproduce the Ewald results accurately. Finally, as a pilot application, we demonstrate that our novel approach can be applied to very large simulation cells (>1 million atoms); results for enthalpies, are presented for a typical non-ideal oxide solid solution (MnO-MgO) as a function of composition and highlight the formation of nano-sized domains in the very large simulation cells. Well defined structures such as exsolution lamellae are not observed.

Introduction

Oxides, both binary and ternary, such as perovskites, have an enormous range of useful properties, exploited in thermoelectrics, ferroelectrics, ion conductors, colossal magneto-resistant materials, superconductors and piezoelectrics and are candidate materials for further uses in energy conversion, in catalysis, as sensors, and in memory applications [1]. The manufacture of working devices often demands the ability to exercise precise control in the industrial production of these materials. Indeed, even atomic level definition may be required for applications such as supported superconductors, magnetic, optical and electronic devices. In order to exercise control during the fabrication process we need to understand the thermodynamic properties and in particular often the subsolidus structure of complex oxide systems. Appreciation of cation ordering, defect clustering, exsolution processes, domain formation and microstructure evolution, and their consequences is crucial both in materials science and in mineralogy.

The literature is awash with relevant examples of which one or two must suffice here. Promising electrolytes for intermediate-temperature solid oxide fuel cells include CeO_2 , doped for example with Gd^{3+} [2]. Simple arguments would suggest that the ionic conductivity would increase steadily with dopant concentration, consistent with an increasing concentration of oxygen vacancies. But the conductivity reaches a maximum at a concentration much before the solubility limit. The traditional explanation is the formation of clusters of the dopant cations and the oxygen vacancies [3,4]. This has been shown to be incomplete by the experimental observation using microscopy and electron diffraction [5] of nano-size domains accompanied by local ordering of oxygen vacancies and dopant segregation, and such domains are also responsible for the decrease in conductivity [6]. But the detailed composition and atomistic structure of the domains, which vary markedly with dopant, and the underlying mechanisms responsible for their formation and influence on the conductivity remain unclear.

Atomistic modelling of such systems in order to tackle these issues is particularly challenging. The length scales involved are such that very large numbers of atoms are needed in simulation cells. Indeed, as pointed out by Wang *et al.* [7], computer

simulations have tended to examine the local structure of point defects and are too small in scale to study nano-domain structure in oxides. Typically such traditional *point-defect* calculations (and thus at the dilute limit) have been carried out to establish the energies of associated defects, such as in recent work on Y-doped CeO₂ [8] where such calculations were used to suggest building blocks for the construction of larger defect clusters. Alternatively, the structure of a large unit cell containing a defect or defect cluster can be optimised (the *supercell* approach) [9]. But such an approach imposes an artificial periodicity, and only a small number of configurations (arrangements) can be considered. Computationally feasible supercells are still too small for microstructure evolution and only a few configurations can be considered. Neither of these methods is readily extended to systems which require explicit consideration of a large number of different configurations over a large lengthscale. We require a method to take explicit account of possible cluster formation and ordering automatically over such lengthscales for specified finite dopant concentrations, making no assumptions about local structure and which can also readily take into account the effects of elevated temperatures.

In previous work we have demonstrated, for oxides and silicates, the use of Monte Carlo (MC) simulations for grossly disordered systems, short-range cation ordering, non-ideal solution solutions, phase equilibria and segregation in thin films and nanoparticles [10, 11, 12, 13, 14, 15, 16]. These are all problems where consideration solely of point defects is insufficient. Nevertheless to date all these simulations have utilised small simulation cells (typically less than a few thousand atoms) and such sizes prevents the analysis of long range order or the microstructure of materials. For example, recent simulations of oxide nanoparticles [17] were unable to show that the properties of the nanoparticle converge with increasing size to those of the bulk since the largest nanoparticles which could be studied computationally consisted only of approximately 22000 ions). When long-ranged forces need not be considered, such as in embedded-atom model simulations of metals, larger lengthscales are now becoming accessible; for example, Erhart *et al.* [18] have modelled atomistically the formation of copper precipitates in α -iron alloys using simulation cells of 786240 atoms. To address similar problems in oxides, there is a need to extend MC simulations which take explicit account of long-range forces to much larger cells.

Molecular Dynamics (MD) is an alternative technique to Monte Carlo for sampling configurational space. MD allows the calculation of time-dependent quantities such as atomic/molecular vibrations and transport coefficients, and algorithms have been developed so that multi-million particle simulations on many thousands of cores are currently routine. These very large MD simulations have largely been achieved by splitting the calculation (both computational and memory requirements) over many processors [^{19,20,21}]. This distributed data strategy allows the simultaneous evolution of the simulation cell on all processors (cores). However MD timescales longer than a few nanoseconds remain a serious problem and the MC method is far more suitable for calculating thermodynamic properties (associated with, e.g. orderings, adsorption, partition coefficients, solvation, self-assembly, agglomeration, melting and crystallization, free energy differences, interfaces). Unfortunately, due to the stochastic nature of MC, it is not straightforward to apply the domain decomposition algorithms developed in MD and this problem is augmented for ionic materials such as oxides, where long-range interactions are necessary. Moreover, in MC simulations it is often necessary to carry out a greater number of moves as the number of particles in the cell increases in order to maintain the same degree of sampling.

In this paper we describe a simple protocol that can be employed to study very large ionic systems using MC style moves. This procedure overcomes many of the limitations in previous calculations and we demonstrate the methodology using a simple binary oxide mixture.

Method

At finite defect or trace element concentrations or in solid solutions it is necessary to sample effectively numerous different configurations, allowing for the exchange of ions at crystallographically inequivalent positions. In standard molecular dynamics simulations of condensed materials kinetic barriers prevent atoms or ions from moving through the lattice and so in almost all cases it is impossible to sample a statistically meaningful number of configurations within a reasonable amount of

computational time. Similarly in Monte Carlo (MC) simulations an unfeasibly large number of random atom displacements are required for an appreciable number of exchanges.

We have previously implemented a MC scheme to calculate the solubility of dopant ions in ionic materials as a function of temperature, pressure and composition [22]. Such MC calculations include four types of change in the system; which type of change is attempted at any stage is made at random.

(i) A random displacement of an ion selected at random. To determine whether the change is accepted or rejected, the usual Metropolis algorithm is applied [23]. The maximum change in the atomic displacement for each ionic species is controlled by a variable r_{max} , its magnitude is adjusted automatically during the simulation to maintain an acceptance/rejection ratio of approximately 0.5.

(ii) A trial change in the cell parameters. All simulations are carried out within the NPT ensemble.²⁴ The magnitude of the volume change is also chosen at random, within a specified amount and is governed by the variable v_{max} (adjusted automatically so that the acceptance/rejection ratio is 0.5). After each volume alteration the change in energy is calculated and a decision whether to accept or reject this is made according to the standard Metropolis scheme. In this study we adjusted only the cell volume, however, the procedure can be generalised (i.e., random changes in any of the lattice parameters).

(iii) Exchange of the positions of two ions selected at random. In our demonstration calculation below, this involves swapping an Mg^{2+} ion and a Mn^{2+} . The change in energy is determined and the exchange is accepted or rejected according to the usual Metropolis method.

(iv) A trial mutation of one cation type into a second type (and *vice versa*) . The energy required for this evaluated and employed to calculate the change in chemical potential.

$$\Delta\mu = -k_B T \ln \left\langle \frac{N_B}{N_A + 1} \exp(-\Delta U_{B/A}/k_B T) \right\rangle, \quad (1)$$

where there are N_A atoms of type A and N_B of type B present in the cell and $\Delta U_{B/A}$. The change in internal energy accompanying the mutation of the B atom into an extra atom A. Note that otherwise N_A and N_B are kept fixed throughout the simulation; this trial mutation is only for calculation of the difference in chemical potential and after this the atom concerned reverts to its original type. Given values of $\Delta\mu$ over a range of compositions, refs. 11-13 show how thermodynamic manipulation then yields free energy differences as a function of composition the phase diagram and the consolute temperature.

Key features of this simulation scheme are the explicit inclusion of the local environments and vibrations (relaxations) of the ions within the simulation, the ease of sampling many different arrangements of cations (configurations).

The accuracy of any simulation is dependent on the suitability of the interatomic potential model chosen. As in our previous calculations we have employed the ionic model writing the interaction energy between any pairs of ions i and j as:

$$U_{ij} = A \exp\left(\frac{-r}{\rho}\right) - \frac{C}{r_{ij}^6} + \frac{q_i q_j}{r_{ij}} \quad (2)$$

The first two terms on the right hand side together form an interatomic potential of the Buckingham form and the potential parameters, A , ρ and C can be obtained through fitting to either *ab initio* or experimental data. For all the calculations presented in this paper we use the potential set developed by Lewis and Catlow [25]. We have previously successfully employed this potential set to study $Mg_{1-x}Mn_xO$ in bulk materials, surfaces and thin films [10,16]. The final term on the right-hand side is the Coulomb interaction of the ions which decays very slowly as a function of distance (as $1/r_{ij}$). As a result special methods have been developed to calculate the electrostatic potential such as the Ewald technique [26], in which the algorithm is restructured so that the summation is split into a reciprocal space and a real space summation. The reciprocal space calculation requires the summation over a large number of reciprocal lattice vectors and, unlike MD in which all the ions are moved simultaneously, impacts considerably on the parallelisation

strategies available for large scale MC simulations. Consequently a domain decomposition strategy for MC has mostly been limited to systems containing only short-range interactions [e.g. . We note that a non-Ewald-based ^{27]} algorithm involving a local approach to the evaluation of electrostatic interactions, in which these are not treated as instantaneous but mediated by a diffusing and constrained electric field on an interpolating lattice, has been proposed by Maggs ^[28] and used by Rottler and Maggs ^[29] and Fahrenberger and Holm³⁰ in MC simulations.

More recently several alternatives have been proposed that allow the electrostatic contribution to the total energy to be calculated simply as a pairwise interaction ^[31, 32, 33]. Fennel and Gezelter, hereafter referred to as FG, have proposed the use of a damped and shifted potential, U_{FG} ,

$$U_{FG} = q_i q_j \left[\frac{\text{erfc}(\alpha r)}{r} - \frac{\text{erfc}(\alpha R_c)}{R_c} + \left(\frac{\text{erfc}(\alpha R_c)}{R_c^2} + \frac{2 \alpha \exp(-\alpha^2 R_c^2)}{\pi^{\frac{1}{2}} R_c} \right) (r - R_c) \right], r \leq R_c \quad (3)$$

where α is a damping parameter. The damping function serves to accelerate the convergence of the Madelung energy to the correct energy as the pairwise interaction cutoff (R_c) distance is increased [30]. The advent of these methods permits the calculation of the electrostatic terms in the same section of the program as the non-bonded pair interactions. Vlught et al. [31] have recently explored the application of both the Wolf and FG methods for the calculation of the thermodynamic properties of small molecules in zeolitic materials. They found that in order to reproduce the thermodynamic data calculated using the Ewald method to the same accuracy, R_c had to be as large as 20 Å ^[34]. Thus for MC simulations using either serial or a replicated data parallel calculation method, the increased cutoff gives rise to a much larger cell size than would be required using the Ewald method negating any computational advantages.

We now present the parallelisation strategy for the MC simulation of multi-million atom simulations. The memory requirements of these simulations and the need to speed up the evaluation of the interaction energy of a particle (to increase the number of configurations sampled within a reasonable time frame) makes it necessary to split the calculation over a number of cores, i.e. domain decomposition is required. This can only be achieved in MC if the domains do not interact and each processor can work on a domain simultaneously. A number of strategies have been developed to prevent the interaction of domains [35]. All of these reduce the domains into subdomains and we followed the approach employed by Shim and Amar in their synchronous relaxation algorithm (figure 3) [36]. This method prevents domain interaction by further subdividing the domain into a core, “skin” and “ghost” regions (subdomains). MC moves within the cores are independent of moves within the adjacent cores. The skin atoms occupy positions where there are possible interactions with the neighbouring core atoms. The ghost atoms reside within neighbouring domains and are necessary to account for all the interactions of the core region.

The size of the skin and ghost subdomains must be greater than $R_c + 2r_{max}$, where $2r_{max}$ is a buffer size, which we set to be 1 Å. In order to prevent two atoms in adjacent domains moving so that their distance is less than R_c . Communication between domains was undertaken with the Message Passing Interface (MPI) [37]. Because of the very large value of R_c in our simulations (see below) the number of ions within a domain could be very large (approximately 10,000 - 27,000 ions if the skin interactions are included). Since the calculation of all these interactions can be very time consuming we used OpenMP [38] within each domain.

The simulation proceeds by selecting at random one of four moves. (i) an attempted move of all the atoms in a subdomain [39, 40] followed by (ii) attempts to exchange the types (positions) of ions within a core subdomain, (iii) —and— an exchange of types (positions) between the core subdomain of different domains or (iv) an attempted change in cell volume. Within the domain decomposition framework the values of r_{max} and v_{max} are stored globally (for r_{max} an average over the cores is calculated). As they

are computed infrequently (approximately every 100 cycles) this does not add significantly to computational time required for the simulation.

Pilot application to solid solutions

We first compare the results obtained with the FG method with a benchmark. For this we used the Ewald technique as implemented in the MC program DL_MONTE [41]. Moreover, DL_MONTE was employed to verify, where possible, the results calculated with the new DDMC code. It is also necessary to establish a framework in which the comparisons can be made. For example, it is not appropriate to use the defect energy of an isolated Mn^{2+} ion in MgO – the difference between two large quantities>> - due to the fluctuations in the total energy during MC simulations and more sensitive tests are required. We found the most useful test was the calculation of the chemical potential difference, $\Delta\mu$, calculated using the test particle mutations described above (equation 1). $\Delta\mu$ was calculated using a 4096 and 216000 atom cells for the DL_MONTE and domain decomposition simulations respectively (for these test calculations we used 8 domains). For all the test simulations the temperature was set to 800 K and tThe cell compositions were $x_{\text{Mn}} = 0.25, 0.5$ and 0.75 . In figure 2 we show the difference in $\Delta\mu$ calculated using the Ewald and FG methods for $x_{\text{Mn}} = 0.25$. The calculations were undertaken for three different values of R_c (12, 15 and 18 Å) and five different values of α (0.1, 0.2, 0.3, 0.4 and 0.5). Figure 2 demonstrates that a large value of R_c is required and α should be set to a value between 0.2 and 0.3. This is in agreement with the conclusions of references 30 and 31. In all our subsequent simulations we use an 18 Å cutoff and set α to 0.25.

A key thermodynamic quantity behind mixing or exsolution in solids is the excess enthalpy of mixing (ΔH_{mix}). Calculated values of ΔH_{mix} using both the Ewald and FG methods are presented in figure 3 and are identical (within statistical uncertainty).

Having demonstrated the accuracy of the FG summation, we now employ it in the DDMC method for the calculation of thermodynamic properties of ionic materials, using

very large simulation cells. We have undertaken a pilot study of the MgO-MnO solid solution with simulation cells containing 1728000 ions. All simulations were run for 10^7 cycles which included 10^9 attempted exchanges of positions (on average approximately 1000 per cation). All the calculations were undertaken on an IBM idataplex using 64 nodes and 16 cores within each node. Such large cells allow us to examine the resulting structures for features such as exsolution lamellae, the formation of which was effectively precluded by the much smaller sizes considered previously. We have calculated the structure over a range of temperatures, at 400, 600 and 800 K, which are below the critical temperature, T_C , calculated from the values of $\Delta\mu$ and at 1400 K, above T_C . In figure 4 we present resulting snapshots of the nano-structure of $\text{Mg}_{1-x}\text{Mn}_x\text{O}$ mixtures for $x = 0.10, 0.25, 0.5$ and 0.75 at 600 K. For the Mg^{2+} rich mixture ($x = 0.10$) the Mn^{2+} ions are often isolated (i.e. next nearest neighbours are Mg^{2+}). However a significant number are associated with other Mn^{2+} ions to form linear chains (often only a single atom in width) in the $[110]$ direction. As the Mg^{2+} concentration decreases, $x = 0.25$, the Mn^{2+} ions are mostly clustered into domains. The domains are strongly asymmetric (they are often only 2-3 cations in diameter and orientated along the $[110]$ direction. We have not observed the formation of well-defined structures such as exsolution lamellae. For $x = 0.5$ these domains have coalesced to form a three dimensional ($>$ than 3 atoms in width) interlocking structure. The final frame in figure 4 is for a composition where the number of larger Mn^{2+} ions exceeds that of the smaller Mg^{2+} ions ($x = 0.75$). The Mg^{2+} ions now form clusters of defects arranged in a linear fashion along $[110]$, similar to those formed by Mn^{2+} at $x = 0.25$.

We have also briefly investigated the influence of temperature on the formation of defect clusters. As expected the association of dopant ions is reduced so that for $x = 0.1$ the dopants tend to be dispersed at temperatures above 600 K. Nevertheless, even at 1400 K for higher concentrations, such as for $x = 0.25$ shown in figure 5, nano-sized domains persist.

Conclusions

We have demonstrated that it is feasible to employ DDMC to study large ionic systems using approximate methods for the long-range Coulomb sum whilst retaining the accuracy of the thermodynamic properties of the materials. This approach is facilitated by the structure of modern high performance computers by providing a combination of MPI and openMP parallelisation.

In this instance we have studied 1728000 ions using 64 domains, but the method could be readily employed to run much larger systems. The technique has been applied in a pilot project to study the structure of $\text{Mg}_x\text{Mn}_{(1-x)}\text{O}$. In these calculations we observe the formation of linear, nano-domains that are orientated along the [110] vector. Well defined structures such as exsolution lamellae are not seen. The size of the domains are such that one should be careful when drawing conclusions from calculations very small simulation cells, especially from the results of ab initio calculations where the computational overheads prevent the use of large cells. Indeed, the use of large simulation cells allows us to investigate previous assumptions regarding the convergence of enthalpies and entropies of mixing with unit cell size, calculated either from Monte Carlo simulations using smaller cells [15] or from configurational averaging of the results from direct free energy minimisation of even smaller cells [42].

Acknowledgements

We acknowledge the use of Hartree Centre resources. The STFC Hartree Centre is a collaborator in association with IBM providing high performance platforms funded by the UK's investment in e-infrastructure. Figures 4 and 5 were produced with Jmol [43].

Figure 1. A two dimensional diagram demonstrating the synchronous relaxation method. The core region is surrounded by the skin (dark grey) and the ghost region (atoms on the neighbouring domain) in light grey. The domains are bounded by the black lines.

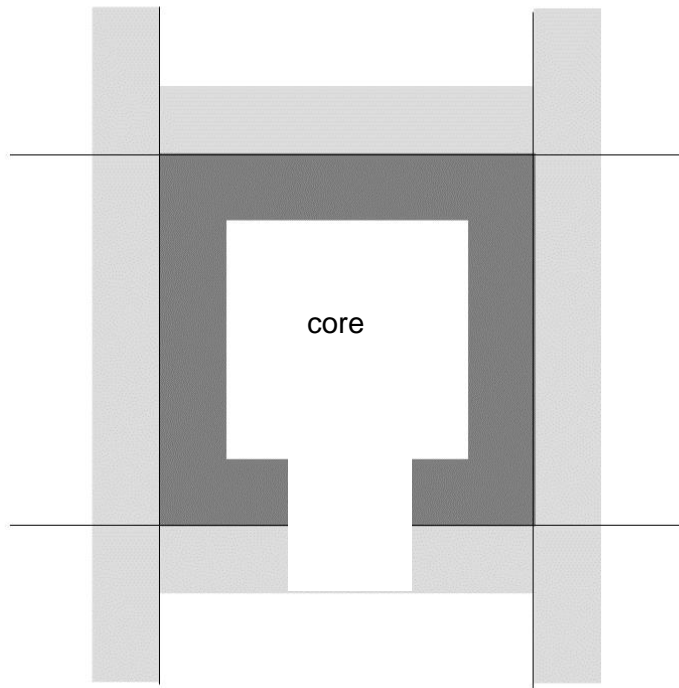


Figure 2. The variation of Δ , the difference in values of the chemical potential change, $\Delta\mu$, calculated with the Ewald and FG methods, with the damping parameter α (equation 3). Results are presented for different values of the pairwise interaction cutoff R_c used in the FG method.

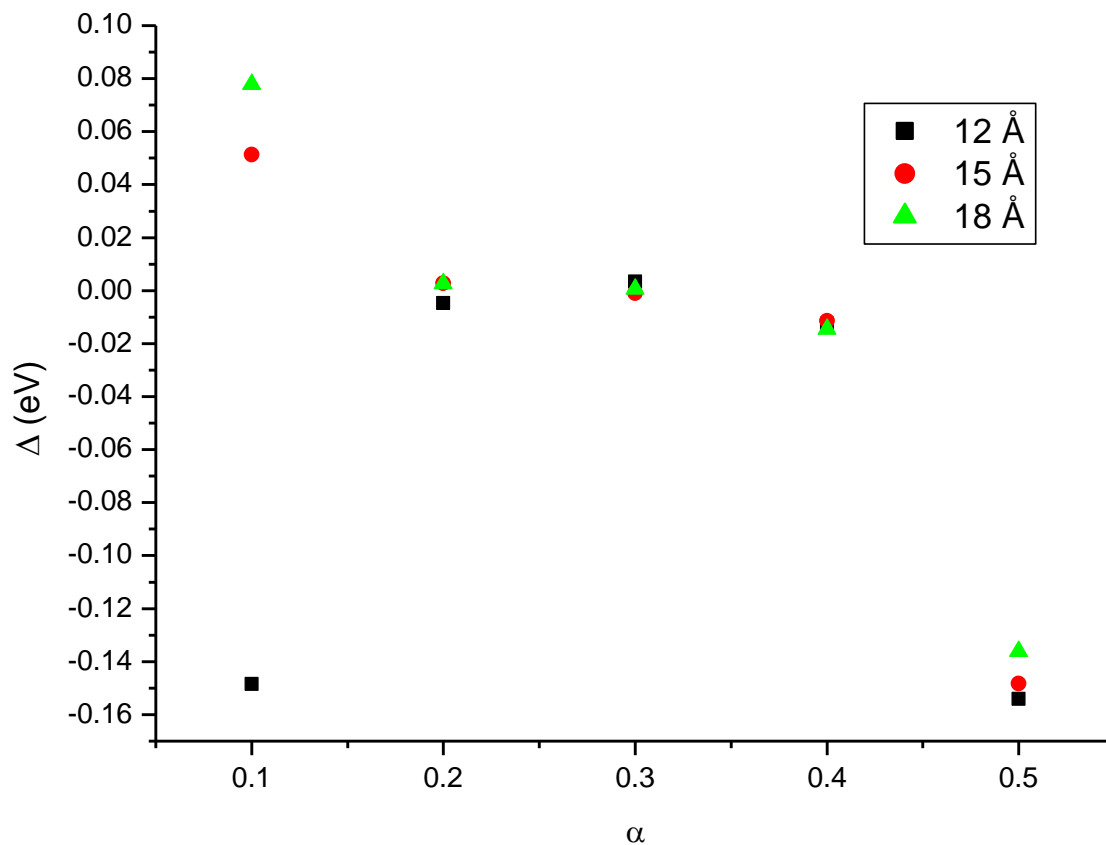


Figure 3. The calculated enthalpy of mixing, ΔH_{mix} , $\text{Mn}_x\text{Mg}_{1-x}\text{O}$, calculated using both the Ewald and FG methods. In the FG calculations, α was set to 0.25 and R_c to 18 Å. The uncertainty in each value of ΔH_{mix} is approximately 0.3 kJ mol⁻¹ for both sets of calculations.

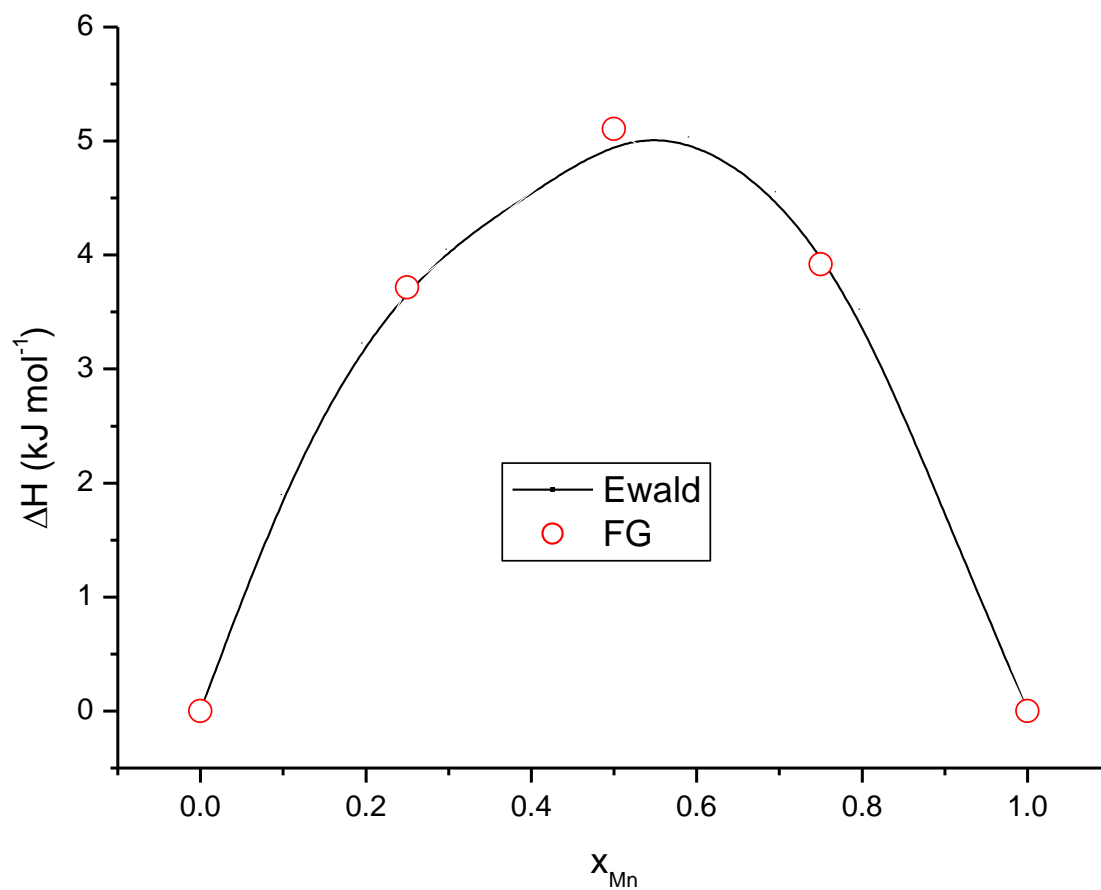
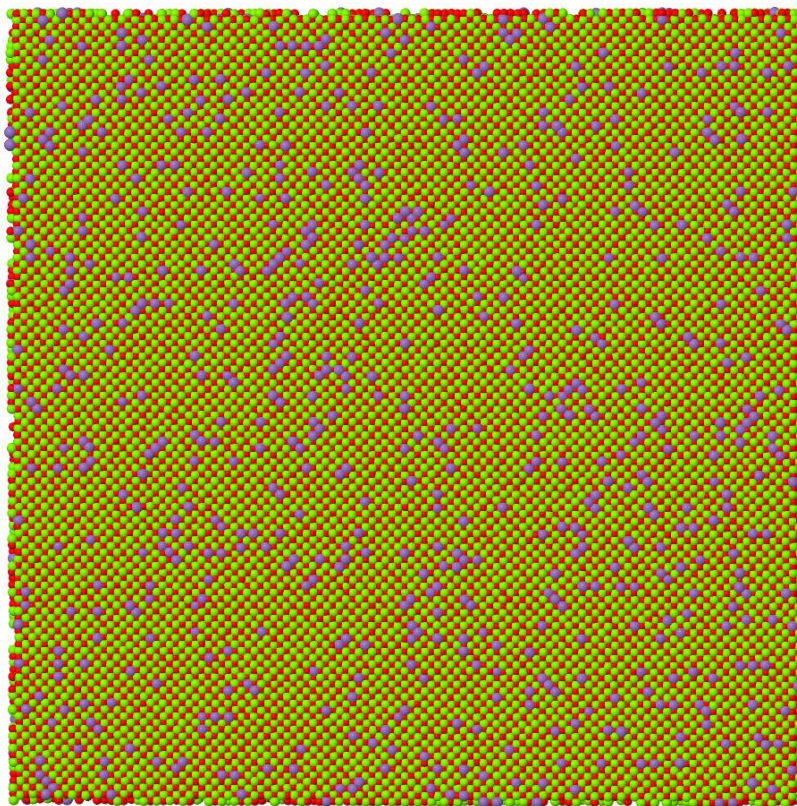
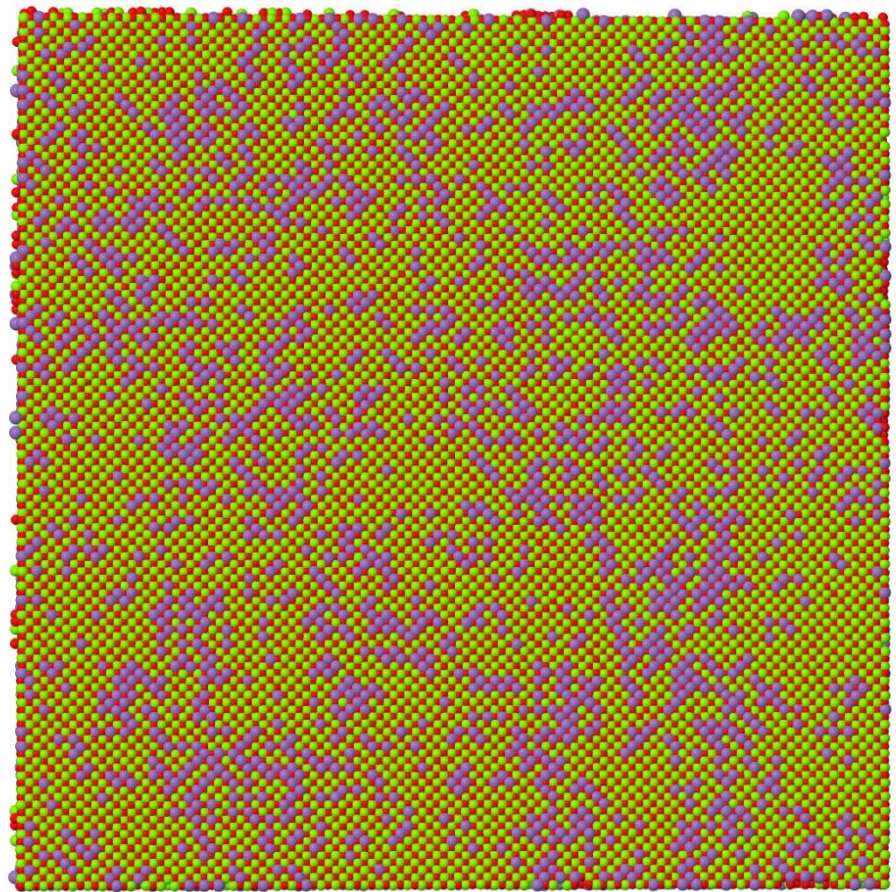


Figure 4. A slice through the cell obtained from DDMC simulations for $\text{Mg}_{1-x}\text{Mn}_x\text{O}$ containing 1728000 ions. a) $x = 0.10$, b) $x = 0.25$, c) $x = 0.5$ and d) $x = 0.75$. All calculations were performed at 600 K which is below the critical temperature for all compositions. Red = oxygen, green = Mg and purple = Mn.
a)



b)



c)



d)

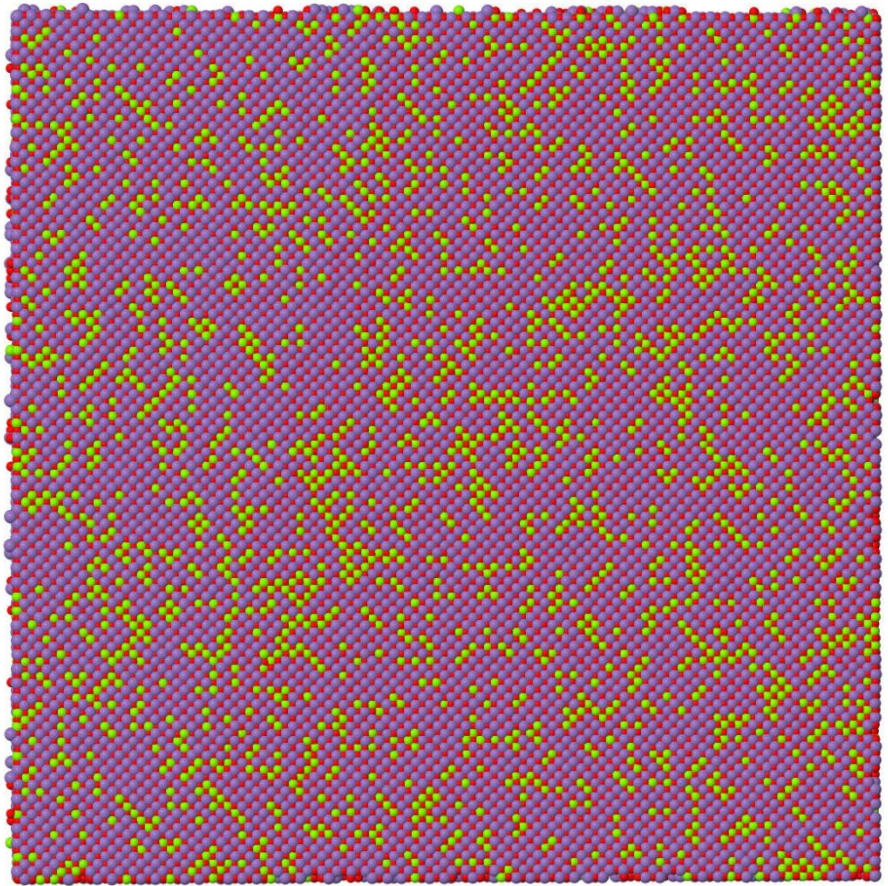
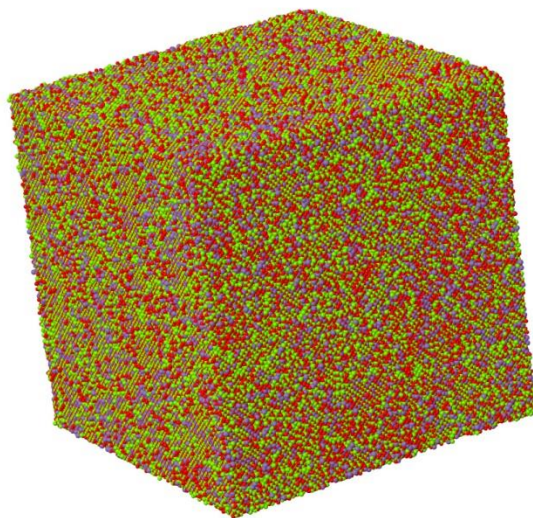


Figure 5. A snapshot of the simulation cell obtained from DDMC simulations for $\text{Mg}_{1-x}\text{Mn}_x\text{O}$, $x = 0.25$, containing 1728000 ions at $T = 1400\text{ K}$ Red = oxygen, green = Mg and purple = Mn.



REFERENCES

- 1 F.M. Granozio, , *MRS Bulletin*, 38:1019 (2013).
- 2 F. Ye, T. Mori, D.R. Ou, J. Zou, G. Auchterlonie, J. Drennan, *Solid State Ionics*, 179: 827, 2008.
- 3 D.Y.Wang, D.S. Park, J. Griffith, A.S. Nowick, *Solid State Ionics* 2 (1981) 95,
- 4 H. Inaba, H. Tagawa, *Solid State Ionics* 83 (1996) 1)
- 5 T. Mori, J. Drennan, Y. Wang, G. Auchterlonie, J.G. Li, A. Yago, *Sci. Technol. Adv. Mater.* 4 (2003) 213
- 6 D.R. Ou, T. Mori, F. Ye, T. Kobayashi, J. Zou, G. Auchterlonie, J. Drennan, *Appl. Phys. Lett.* 89, 171911, 2006
- 7 B. Wang, R.J. Lewis and A.N. Cormack, *Solid State Ionics*, 182:8, 2011.
- 8 Z-P Li, T. Mori, F. Ye, D. Ou, G.J. Auchterlonie, J. Zou and J. Drennan, *J. Phys. Chem., C*, 116, 5435-5443, 2012)
- 9 M.B. Taylor, G.D. Barrera, N.L. Allan, T.H.K. Barron and W.C. Mackrodt, *Faraday Discuss* 106, 377, 1997).
- 10 J.A. Purton, G.D. Barrera, N.L. Allan and J.D. Blundy, *J. Phys. Chem.* **B102**, 5202-5207 (1998)
- 11 M. Yu. Lavrentiev, N.L. Allan, G.D. Barrera, and J.A. Purton, *J. Phys. Chem. B* **105**, 3594–3599 (2001)
- 12 N.L. Allan, G.D. Barrera, M. Yu. Lavrentiev, I.T. Todorov and J.A. Purton, *J. Mat. Chem.* **11**, 63-68 (2001)
- 13 M. Yu. Lavrentiev, N.L. Allan and J.A. Purton, *Phys. Chem., Chem. Phys.* **5**, 2190-2196 (2003);
- 14 M. Yu. Lavrentiev, J.A. Purton and N.L. Allan, *Am. Miner.* **88**, 1522-1531 (2003); see also **89**, 1149 (2004)
- 15 I.T. Todorov, N.L. Allan, M. Yu. Lavrentiev, C.L. Freeman, C.E. Mohn and J.A. Purton, *J. Phys.: Condens. Matter* **16**, S2751-S2770 (2004)
- 16 J.A. Purton, M. Yu. Lavrentiev, N.L. Allan and I.T. Todorov, *Phys. Chem., Chem. Phys.* **7** 3601-3604 (2005)
- 17 J.A. Purton, S.C. Parker and N.L. Allan, *PCCP*, 15:6219, 2013.
- 18 P. Erhart, J. Marian and B. Sadigh, *Phys. Rev. B*, 88:024116, 2013.
- 19 S. Plimpton, *J. Comp. Phys.*, 117:1, 1995.
- 20 G.S. Heffelfinger, *Comp. Phys. Comm.*, 128:219, 2000.
- 21 I.T. Todorov, W. Smith, K. Trachenko and M. Dove, *J. Mat. Chem.*, 16:1911, 2006.
- 22 J. A. Purton, M. Y. Lavrentiev, and N.L. Allan, *Comp. Mat. Sci.*, **105**: 179, 2007.

-
- 23 N.I. Metropolis, A.W. Rosenbluth, M.N. Rosenbluth, A.H. Teller and E. Teller, *J. Chem. Phys.*, 21: 1087, 1953
- 24 D. Frenkel and B. Smit, *Understanding Molecular Simulations: From algorithms to applications*, Academic Press: San Diego, 1996.
- 25 G.V. Lewis and C.R.A. Catlow, *J. Phys. C*, 18:1149, 1985.
- 26 P.P. Ewald, *Ann. Phys. (Leipzig)*, 64:253, 1921.
- 27 G.S. Heffelfinger and M.E. Lewitt, *J. Comp. Chem.*, 17, 250-265 (1996).
- 28 A.C. Maggs and V. Rosetto, *Phys. Rev. Lett.*, 88:196402, 2002
- 29 J. Rottler and A.C. Maggs, *J. Chem. Phys.*, 120:3119, 2004
- 30 F. Fahrenberger and C. Holm,, <http://arXiv:1309.7859> [physics.comp-ph]
- 31 D. Wolf, P. Keblinski, S.R. Philpot and J. Eggebrecht, *J. Chem. Phys.*, 110:8255, 1999.
- 32 D. Zhan, B. Schilling and S.M. Kast, *J. Phys. Chem. B*, 106:10725, 2002.
- 33 C.J. Fennell and J.D. Gezelter, *J. Chem. Phys.*, 124:234104, 2006.
- 34 T.J.H. Vlugt, E. Garcia-Pérez, D. Dubbeldam, S. Ban and S. Calero, *J. Chem. Theory. Comput.*, 4:1107, 2008.
- 35 G.S. Heffelfinger and M.E. Lewitt, *J. Comp. Chem.*, 17:250, 1996.
- 36 Y. Shim and J.G. Amar, *Phys. Rev. B*, 71:115436, 2007
- 37 www.openmpi.org
- 38 <http://www.openmp.org/wp>
- 39 R. Ren and G. Orkoulas, *J. Chem. Phys.*, 126:211102, 2007.
- 40 C.J. O’Keefe, R. Ren and G. Orkoulas, *J. Chem. Phys.*, 127:194103, 2007.
- 41 J. A. Purton, J.C. Crabtree, S.C. Parker, *Mol. Sim.*, 39:1240, 2013.
- 42 N.L. Allan, G.D. Barrera, R.M. Fracchia, M. Yu. Lavrentiev, M.B. Taylor, I.T. Todorov, and J. A. Purton , *Phys. Rev. B* 63:094203, 2001.
- 43 Jmol: an open-source Java viewer for chemical structures in 3D, <http://www.jmol.org>.